A Morphological Study of HDPE-Blown Films Using Small-Angle X-Ray Scattering

ANUNAY GUPTA, DAVID M. SIMPSON, and IAN R. HARRISON*

Department of Materials Science and Engineering, Polymer Science Program,
The Pennsylvania State University, University Park, PA 16802

SYNOPSIS

Discrete small-angle X-ray scattering (SAXS) has been used as an analytical tool to study the development of crystalline morphology in a series of blow-extruded high-density polyethylene (HDPE) films. Processing parameters, take-up ratio (TUR) and blow-up ratio (BUR), were the primary variables used in this investigation. Results from SAXS have led to the consideration of a new microstructural model for crystallite development in blown films. The model incorporates row-nucleated lamellae, where crystalline morphology is sensitive to TUR and BUR. Increasing TUR results in an increase in the number of lamellae in a particular stack, a decrease in fluctuations of amorphous and crystalline thickness distributions, a flattening out of undulations of crystal surfaces, and an increase in the lateral dimensions of lamellae. Increasing BUR did not significantly influence any of the SAXS parameters studied; this can be attributed to the low BURs at which the films were made. © 1993 John Wiley & Sons, Inc.

INTRODUCTION

Polymeric films for high-altitude balloon applications are typically made from low-density polyethylene (LDPE) or linear LDPE (LLDPE) by a blown-film process that applies a biaxial deformation. Films made from blends of LLDPE and high density polyethylene (HDPE) have also been studied as possible candidate materials.[1] A primary criterion for desirable end-use properties is achievement of an appropriate structure that will provide the necessary structural integrity to the film for use in conditions involving low temperature and high flexure.

Discrete small-angle X-ray scattering (SAXS) has proved to be a valuable tool in characterization of crystalline structure in polymers because generally it depends only on large-scale (50–1000 Å) periodic heterogeneities in the structure and is independent of short-range (1–8 Å) arrangement of atoms.[2-4] SAXS patterns from melt-crystallized isotropic polymers typically display a strong first-order diffraction ring and one or two higher orders of much lower intensity. These diffraction rings are a consequence of the regular alternation of crystalline and amorphous regions that have different electron densities. A distribution in repeat distances, as with a distorted crystal, leads to a smearing out of the higher order reflections. Another effect that may lead to the absence of higher order reflections is the nature of the repeat itself. Because in most polymers crystallinity is on the order of 40–60%, crystalline and amorphous phases are of a similar size. Under these conditions very little intensity is scattered to the higher orders, and hence only a limited number of orders are visible.[5] Fluctuations in thickness of crystalline and amorphous components results in imperfect periodicity (paracrystallinity) and hence broad diffraction peaks. Other sources of peak broadening are the finite size of the stack and instrumental constraints (finite size of main beam and finite thickness of sample).

Direct application of Bragg's Law to the maxima ($2\theta_1$) of the Lorentz-geometric corrected scattering curve yields the long period L, where L is the averaged sum of the crystal thickness (L_c) and the amorphous thickness (L_a) in the usual two-phase model. For randomly oriented samples, the Lorentz-

* To whom correspondence should be addressed.

Journal of Applied Polymer Science, Vol. 50, 2085–2093 (1993)
 CCC 0021-8995/93/122085-09

geometric correction is applied to correct for different probabilities of planes being in the reflecting condition.[3,6] At low angles, the combined Lorentz-geometric correction takes the form of a θ^2 multiplicative factor and the effect is to shift maxima to slightly higher angles. Other parameters of interest include P, the reduced full-width at half maximum intensity (FWHM) of the first maxima[7]; N, the number of orders visible; M, the maximum intensity of the first maxima; the deviation from the theoretical value of 2.0 of the ratio of scattering angles from successive maxima, $2\theta_2/2\theta_1$; and Q, the integrated intensity of the scattering curve from $2\theta = 0$ to the angle where the intensity of small-angle scattering becomes zero. Q is frequently referred to as the scattering power of the specimen and is empirically given by the relation,[8]

$$Q = k \cdot V_a V_c \cdot (\rho_c - \rho_a)^2 \qquad (1)$$

where k is a constant, V_a and V_c are the volume fractions of crystalline and amorphous regions, respectively, and $(\rho_c - \rho_a)^2$ is the square of the difference in electron densities between crystalline and amorphous regions. In general, at constant crystallinity, the more perfect the periodicity and the greater the number of crystal lamellae in a particular stack, the smaller the value of P, the reduced FWHM, and the larger the value of N, the number of orders visible and M, the maximum intensity of the diffraction peak.[7] The scattering power Q remains invariant at constant crystallinity irrespective of the morphology of crystal lamellae.

For oriented polymers, such as those made by drawing melt-crystallized polymers at high temperatures, SAXS typically displays strong two-point patterns with maxima in the draw direction or at right angles to the large lateral dimensions of crystal lamellae, as shown in Figure 1.[9] In such cases, the corrected FWHM of the intensity distribution along the width of the maxima, W, conveys information about the lateral size of crystal lamellae.[6,10] As with most scattering phenomena, a smaller W indicates longer lamellae, although this is valid only for perfectly oriented systems. Other parameters are obtained from intensity distributions along the meridian of the scattering curves as in the case for isotropic samples. However, use of Lorentz-geometric corrections on scattering curves of oriented polymers has often been debated, a number of authors contending that it is unnecessary for oriented samples.[7,11,12]

The aim of this work was to use SAXS to study crystalline morphology of blown films of HDPE as a prelude to correlating the parameters obtained from SAXS with the mechanical properties of the films. No attempt was made to study the orientation of the unit cell. They have been studied previously by several authors[13,14] using wide-angle X-ray diffraction. Mechanical and other properties of the films discussed here will be dealt with in a separate article.

EXPERIMENTAL

Sample Preparation

The resin used was Dow 12065 HDPE with a density of 0.965 g/cm^3, a $\overline{M_w}$ of 110,000 and a melt index of 0.8 @ 190/2.16. A Killion extruder with a 1.25-in. barrel 24 : 1 length to diameter ratio; and a 2-in. annular die with a die gap of 0.070 in. were used to make films. For this study, two main processing pa-

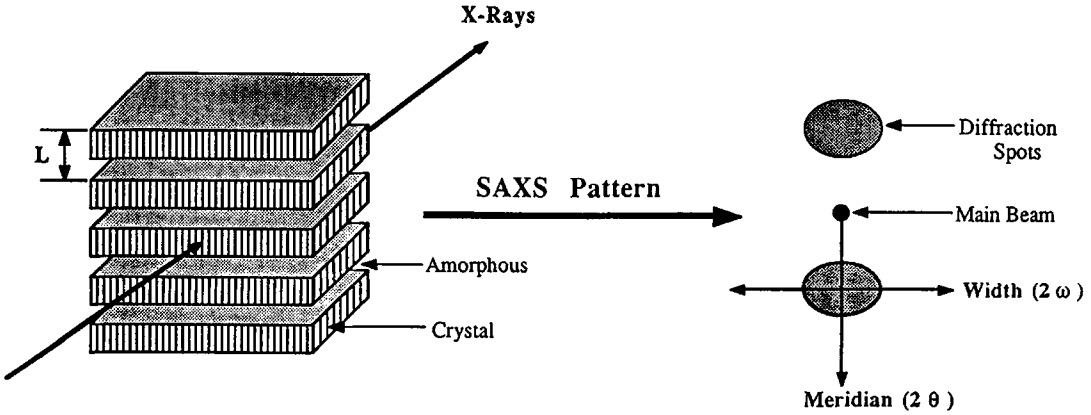

Figure 1 SAXS patterns from oriented crystalline structures. Meridian and width plot directions are marked on the scattering pattern.

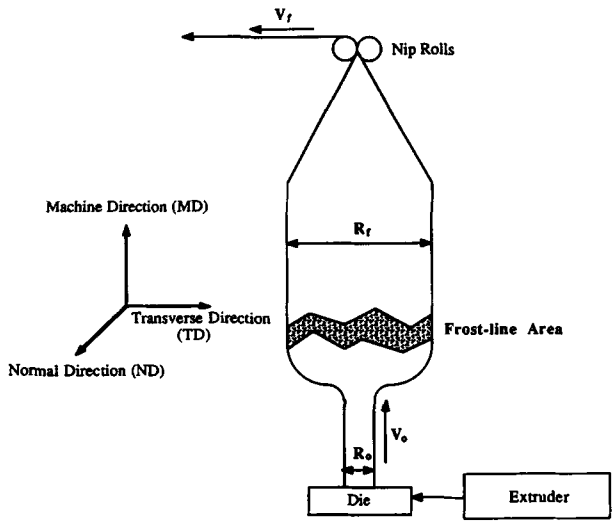

Figure 2 A schematic of the blown-film process with various processing parameters marked out.

rameters were considered: take-up ratio (TUR $= V_f/V_o$) and blow-up ratio (BUR $= R_f/R_o$). Variables are marked in a schematic of the blowing operation in Figure 2. Frostline height (FLH) was kept constant for all films at 12 in. Two sets of samples with varying processing histories were selected for the SAXS analysis: one set (HD-3, 6, 7, 8, and 9) with a constant BUR of 1.7 and TUR increasing from 7.8 to 24.0; and the other (HD-2, 3, 4, and 5) with a constant TUR of 7.8 and a BUR increasing from 1.5 to 2.4. Film thicknesses changed for increasing TUR and BUR because of the interdependence of processing variables. Melt temperatures were held at 243 ± 2°C. A summary of processing conditions is given in Table I.

Thermal Analysis

Two-milligram samples of the HDPE films were heated at 20°C/min from 25 to 175°C in a Perkin–Elmer DSC-7. ΔH_f values were calculated from endothermic peak areas and sample weights. To determine crystallinity, the following relation was used,

$$\% \text{ crystallinity} = \frac{\Delta H_f}{\Delta H_f^\circ} \quad (2)$$

where ΔH_f° was taken to be 301.4 J/g. Percentage crystallinity for all samples are listed along with processing variables in Table I. A variance of ±2% crystallinity was shown in repeated experiments.

Experimental Set-up and SAXS Procedures

All experiments were performed with Cu Kα radiation (λ = 1.5418 Å) with the X-ray generator operating at 40 kV and 35 mA. Monochromatization was achieved using nickel filters and by total reflection of X-rays from two bent nickel-coated mirrors placed at 90° to each other. Bending the nickel-coated mirrors also served to focus the X-ray beam. A three pin-hole collimation unit was used to produce an intense X-ray point source at the detector with minimal parasitic scatter. The FWHM of the main beam at the detector (Δ_m) was measured to be 2.19 mrad 2θ. A two-dimensional solid-state X-ray detector interfaced to a personal computer was used for data acquisition and analysis. The smallest possible scattering angle at which measurements could be made with a high level of accuracy corresponded to a Bragg spacing of ≈500 Å. Sample to detector distance was maintained at 14.15 cm and counting times were typically 3 h. After subtraction of parasitic scatter due to air, all curves were normalized to a common main beam intensity, to a common scattering time and to a constant thickness of sample. Thus, all the curves are directly comparable on an intensity vs. 2θ plot.

Table I Processing Parameters Along With Relevant Properties and SAXS Parameters for HDPE Films

Sample	Blow-Up Ratio (BUR)	Take-Up Ratio (TUR)	Thickness (mil)	Crystallinity (%)	L_1 (±2 Å)	L_2 (±2 Å)	$2\theta_2/2\theta_1$	P (±0.005)
HD-2	1.5	7.8	5.1	68	236	235	2.00	0.616
HD-3	1.7	7.8	4.0	67	236	224	2.10	0.638
HD-4	2.1	7.8	3.7	68	236	223	2.11	0.639
HD-5	2.4	7.8	2.9	67	236	229	2.06	0.684
HD-6	1.7	9.6	3.7	68	235	223	2.11	0.658
HD-7	1.7	12.2	2.6	67	231	222	2.08	0.625
HD-8	1.7	18.0	1.9	66	231	222	2.08	0.603
HD-9	1.7	24.0	1.5	66	220	212	2.08	0.590
Quench	—	—	—	66	242	247	2.04	0.739

Three sets of SAXS experiments were performed for most of the samples. They are shown in Figure 3 in relation to the geometry of their manufacture and are distinguished as SAXS-ND, SAXS-TD, and SAXS-MD; where ND, TD, and MD refer to the three axis of the films, normal direction, transverse direction, and machine direction, along which the X-ray beam was directed. Two types of intensity vs. angle plots, meridian (2θ) and width (2ω), were considered in characterizing film structure, and are shown schematically in Figure 1 in relation to the scattering patterns. All plots thus obtained were normalized and Lorentz-geometric corrected. The following parameters were then calculated:

1. L_1, the long period from $2\theta_1$, the first order of diffraction; and L_2, the long period from $2\theta_2$, the second order of diffraction in Å. The long period L is calculated as

$$2L \sin \theta = n\lambda \tag{3}$$

where θ is half the scattering angle, n is the order of diffraction, and λ is the wavelength of X-rays used.

2. P, the reduced FWHM of the first maxima of the meridian plot. P is calculated as

$$P = \frac{\Delta}{2\theta_1} \tag{4}$$

where $\Delta^2 = \Delta_1^2 - \Delta_m^2$; Δ_1 is the FWHM of the first maxima and Δ_m is the FWHM of the main beam at the detector in 2θ mrad[15];

3. M, the maximum scattered intensity of the first maxima from the normalized uncorrected meridian plots;
4. the ratio $2\theta_2/2\theta_1$ of the scattering angles of the first and second maxima from the meridian plots;
5. Q, the scattering power of the specimen from the meridian plots. Q is calculated as

$$Q = \int_0^\infty I(2\theta)\theta^2 d\theta \tag{5}$$

6. the total integrated normalized intensity over all of reciprocal space; and
7. W, the corrected FWHM of the width plots in 2ω mrad, calculated as

$$W^2 = \Delta_2^2 - \Delta_m^2 \tag{6}$$

where Δ_2 is the FWHM of the width plots and Δ_m is the FWHM of the main beam at the detector in 2ω mrad.

RESULTS AND DISCUSSION

In blown-film extrusion, crystallization occurs over a short period of time and is concentrated in a region typically referred to as the frost-line. Time scales involved are comparable to those in quenching, but unlike normal quenching, polymer crystallizes from the melt while under the influence of a deviatoric stress. This results in the formation of row-nucleated

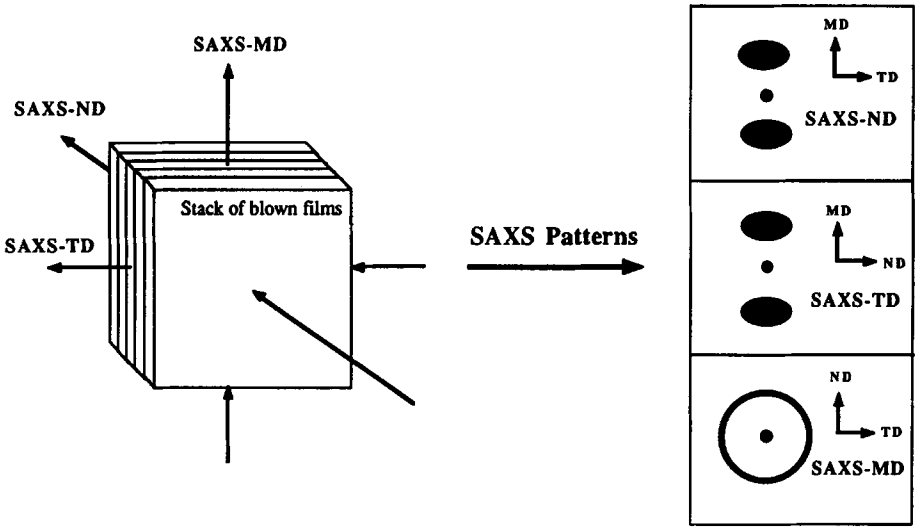

Figure 3 A schematic showing orientation of films for various SAXS experiments and their corresponding patterns.

crystalline structures as opposed to spherulite formation.[16] These structures are formed due to epitaxial crystallization on extended-chain fibrillar crystals that serve as nucleating sites. High TUR prevent rapid relaxation of the extended-chain nuclei, thus ensuring a row-nucleated morphology.

Typical ND, TD, and MD direction SAXS patterns for blown films used in this study are shown schematically in Figure 3. For ND and TD, sharp two-point patterns with negligible scattering on the equator were observed, indicating good orientation of lamellae normals or poles along MD and the absence of extended voids. Similarity in SAXS patterns along ND and TD implies the absence of twisting of lamellae. If indeed the lamellae were twisted, significant departure of SAXS-TD from SAXS-ND should be observed along with considerable arcing in SAXS-TD.[17] Twisting of lamellae in polyethylene has been reported for crystallization under uniaxial stress by Keller and Machin.[16] Their model, based on results from wide-angle X-ray diffraction, incorporates twisting of lamellae at low stress levels; at high stress levels, the lamellae are flat. These observations suggest that for the films studied here, crystallization occurred at high levels of stress.

Four-point patterns often seen in PE specimens that have been drawn or laterally pressed were never observed.[18,19] SAXS patterns along MD gave a much less intense diffraction ring, typical of isotropic melt-crystallized polymers, indicating a small number of isotropically distributed lamellae. Previous orientation studies on blown films using wide-angle X-ray diffraction and birefringence have confirmed the presence of $\approx$5% of unoriented crystalline material.[20] In SAXS-MD, only HD-5, with the maximum BUR showed a very diffuse two-point pattern superimposed on the diffraction ring, indicating the beginnings of orientation of lamellae with normals along TD. It should be noted that discrete scattering in SAXS is only present when there are regular periodic arrangements of lamellae in a stack; isolated, randomly oriented lamellae give rise to diffuse background scattering.

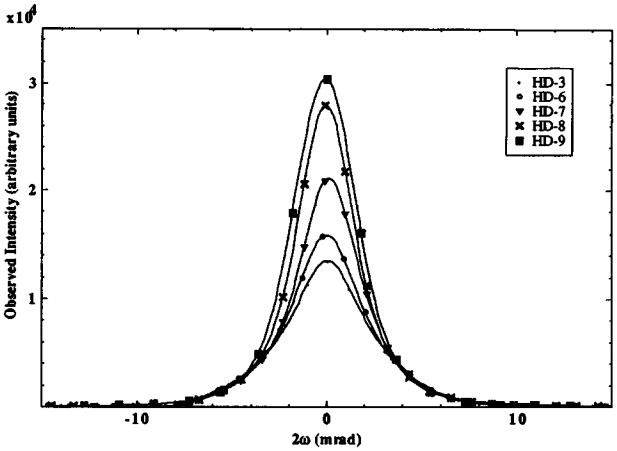

Figure 4(b) Normalized smoothed width plots for HD-3, 6, 7, 8, and 9 along ND.

Normalized smoothed Lorentz-geometric corrected meridian and width plots for samples HD-3, 6, 7, 8, and 9 along ND are shown in Figure 4(a) and 4(b), respectively; corresponding plots for samples HD-2, 3, 4, and 5 are shown in Figure 5(a) and 5(b). A third-order diffraction peak was visible in the original scattering patterns but does not show up in the plots due to its very low intensity. Presence

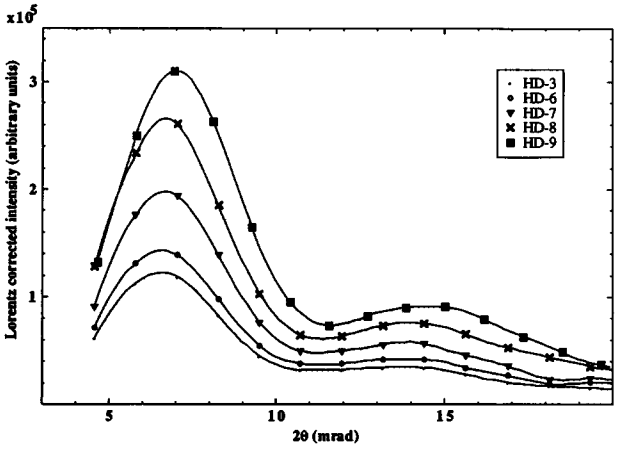

Figure 4(a) Normalized smoothed Lorentz-geometric corrected meridian plots for HD-3, 6, 7, 8, and 9 along ND.

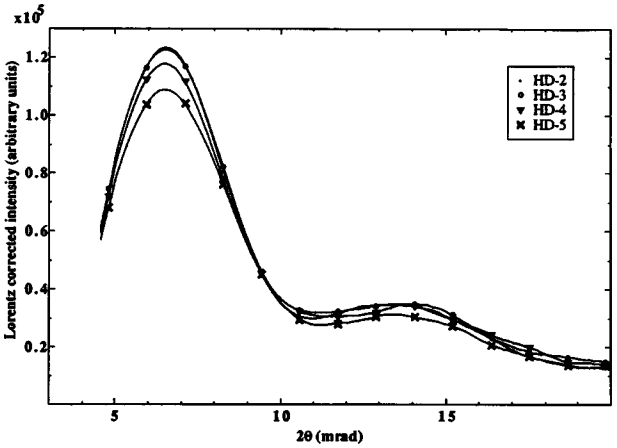

Figure 5(a) Normalized smoothed Lorentz-geometric corrected meridian plots for HD-2, 3, 4, and 5 along ND.

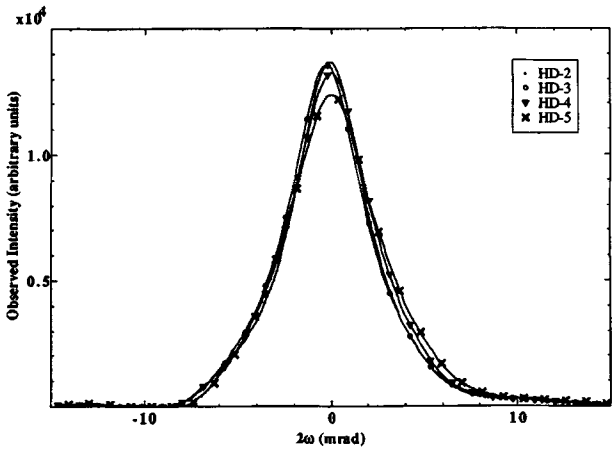

Figure 5(b) Normalized smoothed width plots for HD-2, 3, 4, and 5 along ND.

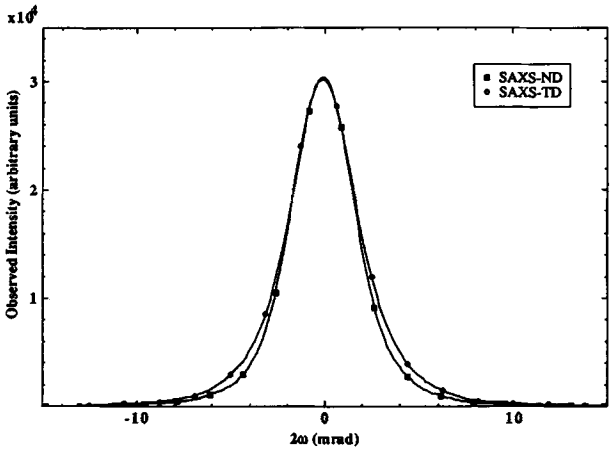

Figure 6(b) Intensity distribution along ND and TD, width for HD-9.

of two or more orders indicates that relative deviations from strict periodicity along the machine direction are less than 15–20%.[21,22] Increasing BUR does not affect morphology as much as increasing TUR. This can be attributed to the small BURs at which the films were made; similar behavior was observed along TD. Figure 6(a) and 6(b) are typical plots of intensity distribution along the ND, TD, and MD for meridian and width plots for HD-9. Similar behavior was observed for all other samples. It is seen that in this case, use of the Lorentz-geometric correction for scattering along the anisotropic ND and TD gives maxima at positions comparable to those obtained from the Lorentz-geometric corrected scattering curve from the isotropic MD. It could be argued that this observation supports application of the Lorentz-geometric correction for oriented samples, although position shifts between corrected and uncorrected maxima are quite small in these samples.

In order to characterize films with regard to development of microstructure, various parameters were calculated. Figures 7–10 show variation of L_1, the long period; P, the reduced FWHM; M, the maximum intensity; and Q, the scattering power for all samples with respect to both TUR and BUR as calculated from meridian plots from SAXS-ND data. Variation of the total scattered intensity is shown in Figure 11. The ratio $2\theta_2/2\theta_1$ was found to vary between 2.0 and 2.1 for all samples and no relation with TUR or BUR was evident. Ratios greater than 2.0 have often been referred to as being due to either the finite size of the transition zone between the crystalline and amorphous regions[23] or positively skewed Reinhold thickness distributions.[24] Parameters L_1, L_2, $2\theta_2/2\theta_1$, and P for all films are listed

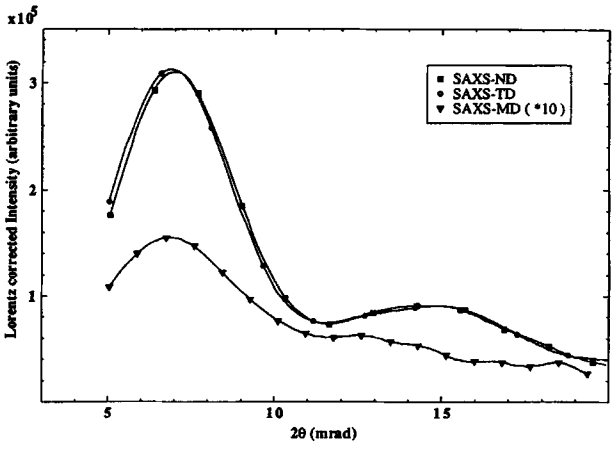

Figure 6(a) Intensity distribution along ND, TD, and MD, meridian for HD-9.

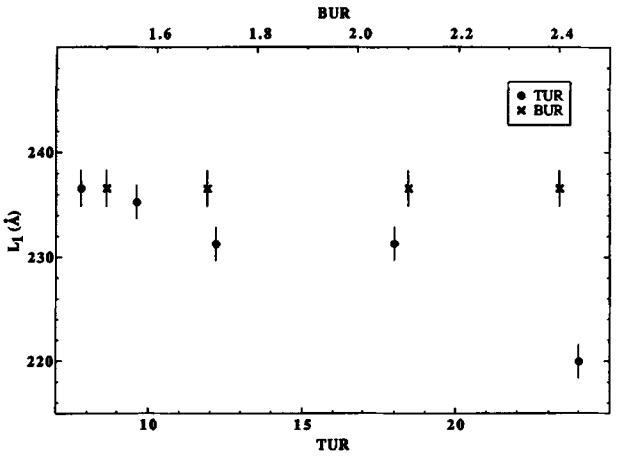

Figure 7 Variation of L_1, the long period with increasing TUR and BUR.

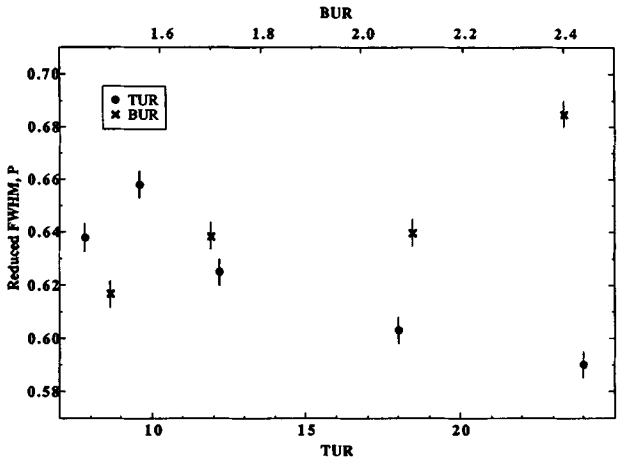

Figure 8 Variation of P, the reduced width with increasing TUR and BUR.

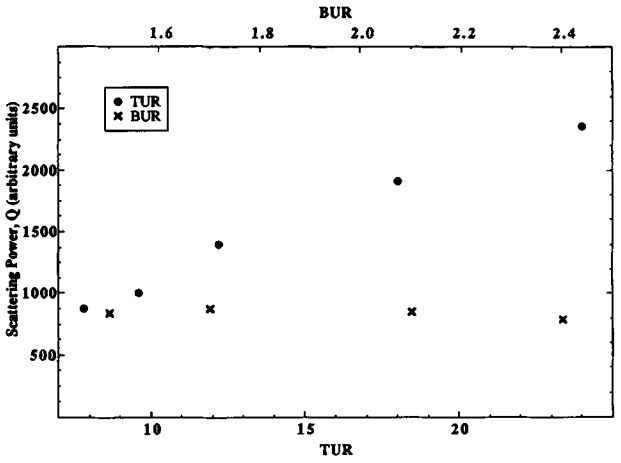

Figure 10 Variation of Q, the scattering power with increasing TUR and BUR.

along with their processing parameters in Table I. Corresponding parameters from a quenched compression-molded HDPE film are also listed for comparison.

An interesting trend is observed in the variation of parameters shown in Figures 7–10 with increasing TUR. There is a decrease in L_1 and in FWHM (P) and a sharp increase in the maximum intensity M, the scattering power Q, and in the total scattered intensity. The decrease in P and increase in M and Q indicate a perfecting of stack structure with more lamellae being incorporated into a stack at higher TUR, and/or a simultaneous decrease of thickness fluctuations of crystalline and amorphous distributions. This is further supported by the strengthening third maxima at higher TUR in the original scattering patterns. However, it is neither possible to unequivocally separate the effects of the two phenomena, nor is it possible to calculate any figures for the number of lamellae in a stack because in all cases, only two maxima showed up in the final plots, with the second order maxima appearing as a shoulder on the first order.

In recent SAXS studies at room temperature that address the variation of scattering patterns for row-nucleated HDPE stretched at 80°C,[25] it was found that as stretch along the machine direction increased, the two-point patterns became diffuse and maxima shifted to lower angles. Lamellar separation, lamellar orientation change, lamellar untwisting, lamellar bending, and chain tilting were identified as the main processes occurring in the deformation process. These observations are in direct contrast to our observations, suggesting the very different development of crystalline morphology in blown films versus row-nucleated films that have undergone hot stretching.

The almost linear increase of scattering power Q

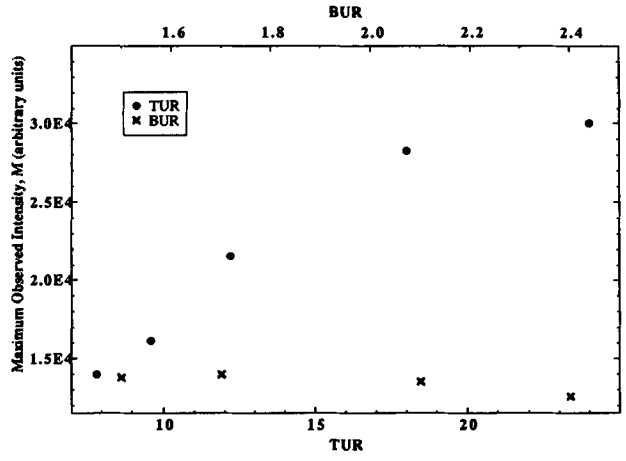

Figure 9 Variation of M, the maximum intensity with increasing TUR and BUR.

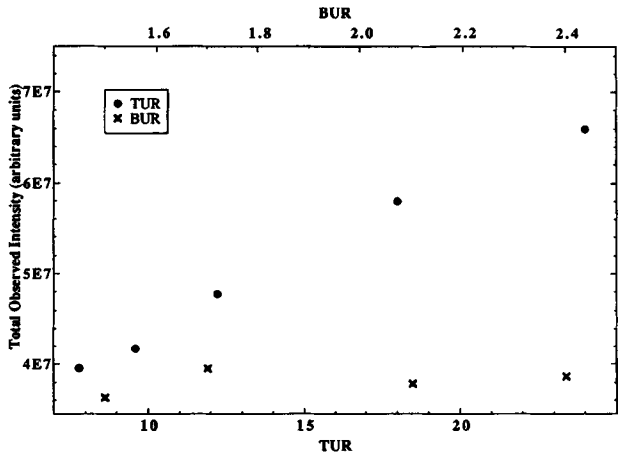

Figure 11 Variation of total scattered intensity with increasing TUR and BUR.

with TUR is puzzling. Percentage crystallinity did not change appreciably in these samples, nor is it likely that an increase in the electron-density difference between crystalline and amorphous phases occurs with increasing TUR. However, randomly distributed stacks of lamellae could get aligned in the machine direction with increasing TUR and isolated crystal lamellae that did not previously contribute to SAXS could be incorporated into periodic structures. However, only the latter case will cause an increase in total scattered intensity, because randomly distributed stacks would have previously contributed to the overall intensity.

To better understand the huge increase in scattering power Q with increasing TUR as compared to increasing BUR, SAXS experiments at three different angles between SAXS-ND and SAXS-MD were carried out. Figure 12 is a plot of the scattering power along the meridian calculated from scattering patterns taken at 0°, 13°, 22°, 45°, and 90° for HD-6 and HD-9. A very steep decline in Q at small angles is seen for HD-9. In contrast, decrease of Q with angle for HD-6 is linear. Furthermore, the area under the two curves is approximately the same suggesting the same amount of crystallinity in both samples. These observations suggest some sort of a flattening out of undulations of crystal surfaces upon increasing TUR.

In contrast to TUR, increasing BUR did not significantly change most of the parameters studied. Perhaps this can be attributed to the small changes in value of BUR at which films were made. However, a slight increase in P was noticed. The presence of a diffuse two-point pattern superimposed on the diffraction ring for HD-5/SAXS-MD indicates the commencement of lamellar orientation with normals parallel to TD. However, none of the other films

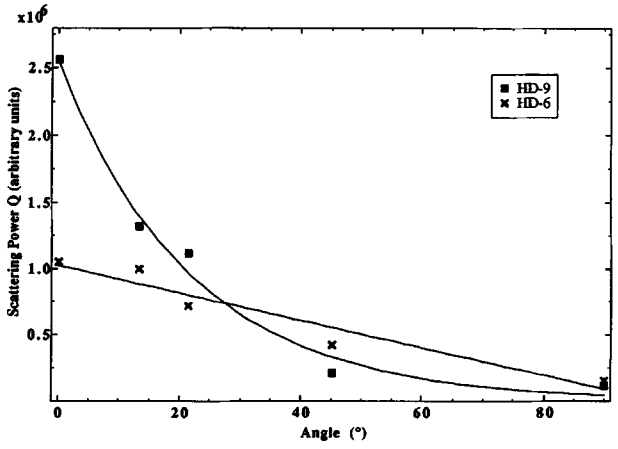

Figure 12 Variation of scattering power Q along meridian with angle between ND and MD for HD-6 and 9.

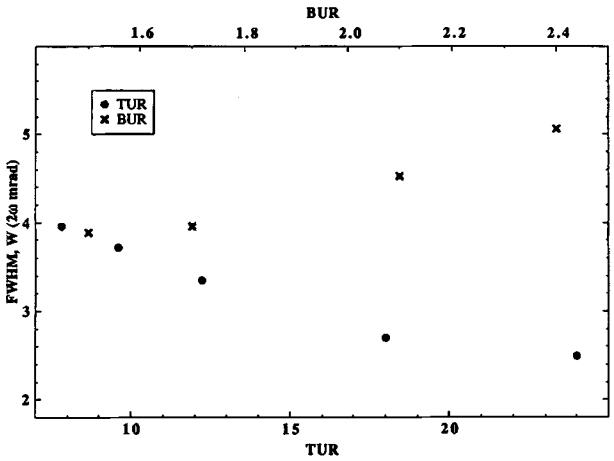

Figure 13 Variation of W, the FWHM obtained from width plots, ND with increasing TUR and BUR.

HD-2, 3, and 4 exhibited this behavior. Therefore it can be said that none of the films studied exhibited true biaxial orientation, with HD-5 showing traces of it.

Figure 13 is a plot of W, the corrected FWHM as obtained from width plots for SAXS-ND. The dramatic decrease in W indicates an increase in size of the lateral dimensions of lamellae with increasing TUR. If it is assumed that W is inversely proportional to the lateral dimensions, an increase of $\approx$100% is noted on going from a TUR of 7.8 to 24. This observation is valid only if lamellae have perfect orientation along the machine direction that appears to be reasonably true for HD-6, 7, 8, and 9 because they exhibited strong two-point scattering patterns with negligible equatorial scattering (after subtracting any scattering due to isotropically distributed lamellae) or arcing. For HD-2, 3, 4, and 5, a sharp increase in W even at the small BURs studied indicates either a shortening of lamellar length or an increasing misorientation of lamellae; the latter appears more likely based on consideration of the manufacturing process.[20] After extrusion through the annular die, both stretching and blow-up occur in the melt before polymer crystallizes at the frost-line. Stretching appears to first orient molecules in the viscous melt parallel to the machine direction; this orientation is subsequently reduced by the blow-up process. However, a net fiber-type orientation is still produced in the machine direction.

CONCLUSIONS

Based on the above observations and discussion, a model for the development of crystalline morphology

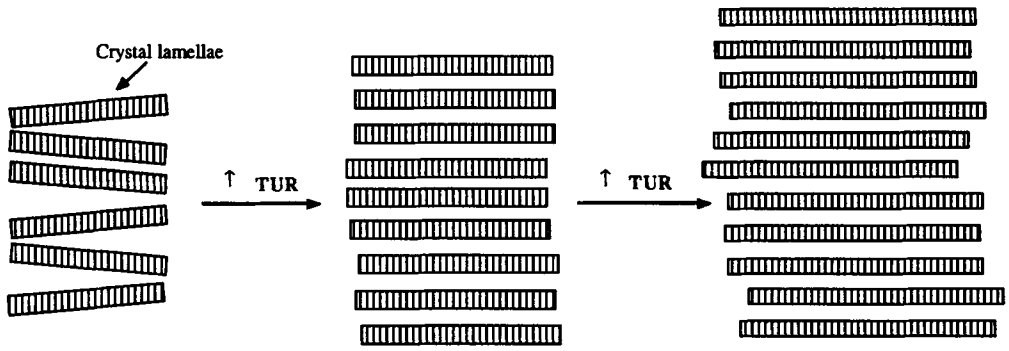

Figure 14 A schematic of the development of crystalline morphology upon increasing TUR.

in blown-HDPE films is proposed. Crystallization under the influence of a deviatoric stress results primarily in the formation of row-nucleated lamellae, whose morphology is very sensitive to the processing parameter take-up ratio (TUR) and blow-up ratio (BUR). As TUR is increased, four phenomena can take place: an increase in the number of lamellae in a particular stack; a decrease in fluctuations of amorphous and crystalline thickness distributions; flattening out of undulations of crystal surfaces; and an increase in the lateral dimensions of lamellae. A schematic of the process is shown in Figure 14. For increasing BUR, biaxial orientation starts developing only at BUR greater than 2.4, although much higher BUR are apparently necessary for a significant number of lamellae to be oriented with normals parallel to TD.

It is hoped that mechanical, thermal, and microscopic (optical and electron) studies on these films will correlate with SAXS parameters and help to establish the veracity of the proposed structures. SAXS experiments similar to those outlined in this paper are currently being carried out on films made from LDPE and LLDPE.

The authors would like to thank NASA Balloon Branch for partial support of this research. One of us (D.M.S.) would also like to thank Amoco for fellowship support during part of this study.

REFERENCES

1. D. M. Simpson, Master's thesis, The Pennsylvania State University, 1991.
2. G. Porod, *Kolloid-Z., Z. Polym.*, **124** (1951).
3. P. H. Debye, R. Anderson, and H. Brumberger, *J. Appl. Phys.*, **28,** 679 (1957).
4. A. Guinier and G. Fournet, *Small-Angle Scattering of X-rays,* John Wiley & Sons, London, 1955.
5. Ian L. Hay, in *Methods of Experimental Physics, Vol. 16: Polymers, Part C,* Chap. 13, R. A. Fava, ed., Academic Press, New York, 1980.
6. L. E. Alexander, *X-ray Diffraction Methods in Polymer Science,* Chap. 5, Wiley-Interscience, New York, 1969.
7. B. Crist and N. Morosoff, *J. Polym. Sci., Polym. Phys. Ed.*, **11,** 1023 (1973).
8. P. H. Hermans and A. Weidinger, *Makromol. Chem.*, **39,** 67 (1960).
9. J. S. Higgins and R. S. Stein, *J. Appl. Cryst.*, **11,** 346 (1978).
10. K. Hess and H. Kiessig, *Kolloid-Z.*, **130,** 10 (1953).
11. Z. Kifle, I. R. Harrison, and R. M. Herman, *J. Polym. Sci., B, Polym. Phys.*, **24,** 633 (1986).
12. J. Dlugosz, G. V. Fraser, D. Grubb, A. Keller, and J. A. O'dell, *Polymer,* **17,** 471 (1976).
13. J. L. White and M. Cakmak, *Adv. Polym. Technol.*, **8,** 27 (1988).
14. A. Keller, *Nature,* **174,** 826 (1954).
15. I. R. Harrison, S. J. Kozmiski, W. D. Varnell, and J. I. Wang, *J. Polym. Sci., Polym. Phys. Ed.*, **19,** 487 (1981).
16. A. Keller and M. J. Machin, *T. Macromol. Sci. (Phys.),* **B1,** 41 (1967).
17. S. J. Pan, J. Im, M. J. Hill, A. Keller, A. Hiltner, and E. Baer, *J. Polym. Sci., B, Polym. Phys.*, **28,** 1105 (1990).
18. E. P. H. Meibohm and A. F. Smith, *J. Polym. Sci.*, **7,** 449 (1951).
19. W. O. Statton and G. N. Godard, *J. Appl. Phys.*, **28,** 1111 (1957).
20. D. R. Holmes and R. P. Palmer, *J. Polym. Sci.*, **31,** 345 (1958).
21. R. Bonart and R. Hosemann, *Kolloid-Z., Z. Polym.*, **186,** 16 (1962).
22. R. Hosemann, *J. Appl. Phys.*, **34,** 25 (1963).
23. B. Crist, *J. Polym. Sci., Polym. Phys. Ed.*, **11,** 635 (1973).
24. C. Reinhold, E. W. Fisher, and A. Peterlin, *J. Appl. Phys.*, **35,** 71 (1964).
25. P. Young, R. S. Stein, and T. Kyu, *J. Polym. Sci., B, Polym. Phys.*, **28,** 1791 (1990).

Received January 26, 1993
Accepted May 27, 1993